

Determination of disordered magnetic structures by RMC modelling of neutron diffraction data

This article has been downloaded from IOPscience. Please scroll down to see the full text article.

1991 J. Phys.: Condens. Matter 3 7383

(<http://iopscience.iop.org/0953-8984/3/38/010>)

View [the table of contents for this issue](#), or go to the [journal homepage](#) for more

Download details:

IP Address: 171.66.16.147

The article was downloaded on 11/05/2010 at 12:34

Please note that [terms and conditions apply](#).

Determination of disordered magnetic structures by RMC modelling of neutron diffraction data

D A Keen† and R L McGreevy‡

†ISIS Science Division, Rutherford Appleton Laboratory, Chilton, Didcot, Oxfordshire OX11 0QX, UK

‡Clarendon Laboratory, Parks Road, Oxford OX1 3PU, UK

Received 17 June 1991

Abstract. We describe how reverse Monte Carlo (RMC) modelling may be used to analyse neutron diffraction data from a disordered magnetic material. By applying the technique to the amorphous binary alloy Dy_7Ni_3 we determine both an atomic structure and a magnetic structure which reproduce the diffraction data. The atomic structure is found to be essentially random close packed while the magnetic structure at low temperatures is dominantly ferromagnetic. The development of short and long range magnetic order can be followed as the temperature is decreased below the Curie temperature. We anticipate that this technique, already employed for the determination of many different types of disordered atomic structures, will also be of great use in the determination of disordered magnetic structures in amorphous and crystalline magnetic materials.

1. Introduction

The magnetic structure of materials which exhibit either long range order or complete disorder are reasonably well understood for systems where the spins lie on regular lattice sites. For systems where these extremes of order/disorder are not displayed, or where the spins lie on an irregular atomic arrangement, the magnetic structures are still not well characterized. Spin glasses (see e.g. Binder and Young 1986, Huang 1985), frustrated magnets such as certain dilute magnetic semiconductors (Furdyna and Samarth 1987), and magnetic amorphous materials (e.g. Moorjani and Coey 1984, Sellmeyer *et al* 1988) all come into this category and because of the wide interest in these materials it would be of considerable value to develop a method for determining their magnetic structure. The above materials show coherent diffuse scattering in their neutron diffraction patterns which is associated with either short range atomic order or short range magnetic order or both. McGreevy and Puzsai 1988 have shown that the reverse Monte Carlo (RMC) method can be used to model the atomic short range order associated with diffuse scattering. The question of the uniqueness of the structures produced by this method has been discussed in detail by McGreevy *et al* 1990 and Howe and McGreevy 1991. In this paper the RMC technique is extended to encompass magnetic diffuse scattering and hence to model the magnetic structure of disordered materials.

Computer simulation methods are not new to the study of disordered magnetism (see e.g. Fernandez and Streit 1982, Fernandez *et al* 1983 and references therein). However, most techniques that have already been employed are based on some form

of exchange interaction, e.g. the RKKY interaction for spin glasses (Ruderman and Kittel 1954, Kasuya 1956, Yosida 1957). By definition a model has therefore been imposed on the resultant magnetic structure. RMC, in contrast, benefits from the fact that no prior knowledge of interatomic (or spin-spin) interactions is required and the model produced is only constrained by the experimental data which is being used. This is especially useful when potentials are either not known or only approximately determined.

This paper is organized as follows: in section 2 we outline the RMC technique and describe how it has been adapted to analyse disordered magnetic systems. In section 3 we apply the technique to neutron diffraction data on amorphous Dy_7Ni_3 measured by Hannon *et al* (1991) using the double-null isotopic substitution technique (Wright *et al* 1984) and in section 4 we discuss the results obtained from the simulation. The final section will contain concluding remarks and a discussion of how the technique may be of use in the general context of disordered magnetic systems where isotopic substitution neutron diffraction measurements may not be possible.

2. Reverse Monte Carlo modelling

RMC is a method for producing three-dimensional models of the structure of disordered materials which agree quantitatively with the available diffraction data. The technique, which is described in detail by McGreevy *et al* (1990), is similar to the Metropolis Monte Carlo method (Metropolis *et al* 1953), with the difference that instead of moving atoms to minimize the potential energy of the system, the difference between the measured structure factor(s) and the calculated structure factor(s) is minimized. Atoms are placed in a box with periodic boundary conditions and moved randomly one at a time to minimize

$$\chi^2 = \sum_k \sum_{i=1}^{m_k} [F_k^C(Q_i) - F_k^E(Q_i)]^2 / 2\sigma_k^2(Q_i) \quad (1)$$

where $F_k^C(Q)$ and $F_k^E(Q)$ are the calculated and experimental structure factors corresponding to the data set k respectively and $\sigma_k(Q)$ is an estimate of the experimental uncertainty. m_k is the number of Q points in data set k . Moves are accepted unconditionally if χ^2 is reduced and are accepted with probability $\exp(-\Delta\chi^2)$ if χ^2 is increased, $\Delta\chi^2$ being the change in χ^2 for that move. All other moves are rejected. Atoms are moved until χ^2 reaches an equilibrium value about which it oscillates. The resulting configuration of atoms should be a three-dimensional structure which is consistent with $F^E(Q)$ within the experimental error σ . Independent configurations are then collected by saving subsequent configurations which are at least N accepted moves apart, N being the number of atoms.

The extension of the RMC technique to modelling disordered magnetic structures is straightforward. The total structure factor for a magnetic material contains terms which have both nuclear and magnetic origin. Spins, μ , are assigned to each magnetic atom in the configuration. The spins are rotated randomly on the atomic positions and the atom positions are also moved randomly in order to minimize χ^2 in the manner described above. The resulting configuration now contains a three-dimensional atomic structure and a three-dimensional spin structure which are consistent with the experimental total structure factor(s) within the experimental error.

The nuclear and magnetic contributions to the neutron scattering intensities are additive for an unpolarized neutron beam (Wright 1980) and the nuclear structure factor may be defined in the usual way as a combination of partial structure factors (Faber and Ziman 1965). The formalism of Blech and Averbach (1964) is used for the calculation of the magnetic structure factor. The differential scattering cross-section of a polycrystalline sample containing only one magnetic species is defined as

$$I_M(Q) = \frac{d\sigma}{d\Omega_M} = \frac{d\sigma}{d\Omega_P} + 4\pi\rho c_M \int r^2 \left[A(r) \frac{\sin Qr}{Qr} + B(r) \left(\frac{\sin Qr}{(Qr)^3} - \frac{\cos Qr}{(Qr)^2} \right) \right] dr \quad (2)$$

where the paramagnetic scattering contribution is

$$\frac{d\sigma}{d\Omega_P} = \frac{2}{3} c_M \left[\frac{e^2\gamma}{2m_e c^2} \mu f_M(Q) \right]^2 \quad (3)$$

c_M is the concentration of the magnetic ion, ρ is the number density of ions, $(e^2\gamma/m_e c^2)^2 = 0.29 \times 10^{-24} \text{ cm}^2$, μ is the magnitude of the magnetic moment (in μ_B) and $f_M(Q)$ is the magnetic form factor.

$$A(r) = \left(\frac{e^2\gamma}{2m_e c^2} \right)^2 f_M^2(Q) \langle \mu_y(\mathbf{0}) \cdot \mu_y(\mathbf{r}) \rangle \quad (4)$$

and

$$B(r) = \left(\frac{e^2\gamma}{2m_e c^2} \right)^2 f_M^2(Q) [2\langle \mu_x(\mathbf{0}) \cdot \mu_x(\mathbf{r}) \rangle - \langle \mu_y(\mathbf{0}) \cdot \mu_y(\mathbf{r}) \rangle] \quad (5)$$

x and y subscripts denote the component of μ parallel and perpendicular to the radius vector joining the atoms at $\mathbf{0}$ and \mathbf{r} respectively.

$\langle \mu \cdot \mu \rangle$ at distance r is defined as

$$\langle \mu \cdot \mu \rangle_r = \frac{n_\mu(r)}{4\pi r^2 dr \rho c_M} - \sum_0^R n_\mu(r) / \frac{4}{3} \pi R^3 \rho c_M \quad (6)$$

where $n_\mu(r)$ is the sum of $\mu(\mathbf{0}) \cdot \mu(\mathbf{r})$ for atoms at a distance between r and $r + dr$ from a central magnetic atom, averaged over all magnetic atoms as centres. R is half the length of the (cubic) configuration box. Clearly $\langle \mu \cdot \mu \rangle_r$ has a similar form to the radial distribution function $g(r)$.

Hence the total structure factor $I^C(Q) = F^C(Q) + I_M^C(Q)$ may be calculated directly from the configuration of atoms and spins. This function is fitted to the corrected experimental data (the nuclear self-scattering having been subtracted) by minimizing χ^2 , where $F^C(Q)$ and $F^E(Q)$ in equation (1) are replaced by $I^C(Q)$ and $I^E(Q)$.

3. Application to Dy₇Ni₃

The neutron diffraction data of Hannon *et al* (1991) on the amorphous alloy Dy₇Ni₃ are especially useful for testing the applicability of RMC since the double-null isotopic

substitution technique was used. In Dy_7Ni_3 the coherent nuclear scattering length \bar{b} of each element may be set to zero by a suitable combination of isotopes. Hence by using samples where one or both elements have $\bar{b} = 0$ as well as a natural isotopic composition sample, not only may the atomic partial correlation functions be readily separated but the magnetic scattering may also be isolated. When both Dy and Ni have $\bar{b} = 0$ the only contributions to the neutron scattering are either structureless incoherent nuclear scattering or magnetic scattering. Four samples were measured by Hannon *et al* (1991) at room temperature; $^{\text{N}}\text{Dy}_7^{\text{N}}\text{Ni}_3$, $^{\text{N}}\text{Dy}_7^0\text{Ni}_3$, $^0\text{Dy}_7^{\text{N}}\text{Ni}_3$ and $^0\text{Dy}_7^0\text{Ni}_3$. $^0\text{Dy}_7^0\text{Ni}_3$ was also measured at $T = 96, 44$ and 7K . The superscript N refers to the natural isotopic combination and 0 to the isotopic combination giving $\bar{b} = 0$. From the four data sets measured at room temperature it is possible to produce three structure factors containing only coherent nuclear scattering; $^{\text{NN}}F(Q)$, $^{\text{N}0}F(Q)$ and $^{0\text{N}}F(Q)$. These were then fitted simultaneously using RMC to produce a configuration of atom positions which described the atomic structure. The initial configuration contained a random distribution of 1000 atoms in the correct proportion in a cubic box with sides $L = 29.39\text{Å}$. Atoms were not allowed to be closer to each other than a certain cut-off distance. These distances were $r_{\text{Dy-Dy}}^0 = 3.1\text{Å}$, $r_{\text{Dy-Ni}}^0 = 2.4\text{Å}$ and $r_{\text{Ni-Ni}}^0 = 2.2\text{Å}$, values determined from direct solution for the partial radial distribution functions. A 1% uncertainty was estimated for the data. The fits to the data sets are shown in figure 1 and display very good agreement. The partial radial distribution functions, $g_{ij}(r)$, calculated from the configuration (figure 2) are in close agreement with those produced by Hannon *et al* (1991) who used conventional separation techniques which are possible with isotopic substitution data (Enderby *et al* 1966).

An advantage of RMC simulation over such separation techniques is that extra information on the structure may be obtained. Since a three-dimensional distribution of atoms consistent with the data is produced, neighbour distributions and three particle correlation functions such as bond-angle distributions may also be calculated. The distributions of number of neighbours within the first co-ordination shell, defined by the first minimum in the appropriate $g_{ij}(r)$ (4.4, 3.3 and 3.6 Å for Dy-Dy, Dy-Ni and Ni-Ni respectively), are shown in figure 3. These give average co-ordination numbers of $C_{\text{Dy-Dy}} = 10.2$, $C_{\text{Dy-Ni}} = 2.5$, $C_{\text{Ni-Dy}} = 5.8$ and $C_{\text{Ni-Ni}} = 1.8$ which are consistent with those obtained by Hannon *et al* (1991) by fitting the first peak in $rg_{ij}(r)$. The bond angle distributions, $P(\cos\theta)$ are shown in figure 4, where maximum bond lengths are again defined by the first minimum in $g_{ij}(r)$.

Having obtained a configuration which describes the atomic structure, attention was then turned to the magnetic structure. The neutron diffraction pattern of $^0\text{Dy}_7^0\text{Ni}_3$, due only to magnetic scattering, displays an increasing amount of structure as the temperature is reduced. Assuming that the Ni moments are quenched (Buschow 1980), that the moment on the Dy^{3+} ion is constant with the free ion value of $10.6\mu_{\text{B}}$ (Kittel 1976) and using the calculated values for the Dy^{3+} ion form factor (Lisher and Forsyth 1971), these data sets were also fitted using RMC. A spin was placed on each Dy atom position in the configuration and these spins were rotated randomly one at a time until χ^2 converged. The atom positions were kept fixed, since they had already been determined from the room temperature data sets. Small temperature dependent effects on the nuclear structure were not taken into account. The $^0\text{Dy}_7^0\text{Ni}_3$ data sets had not been normalized and hence it was necessary to introduce a scaling and additive constant in the model which were determined automatically within the RMC procedure (McGreevy *et al* 1990). A perfect ferromagnetic

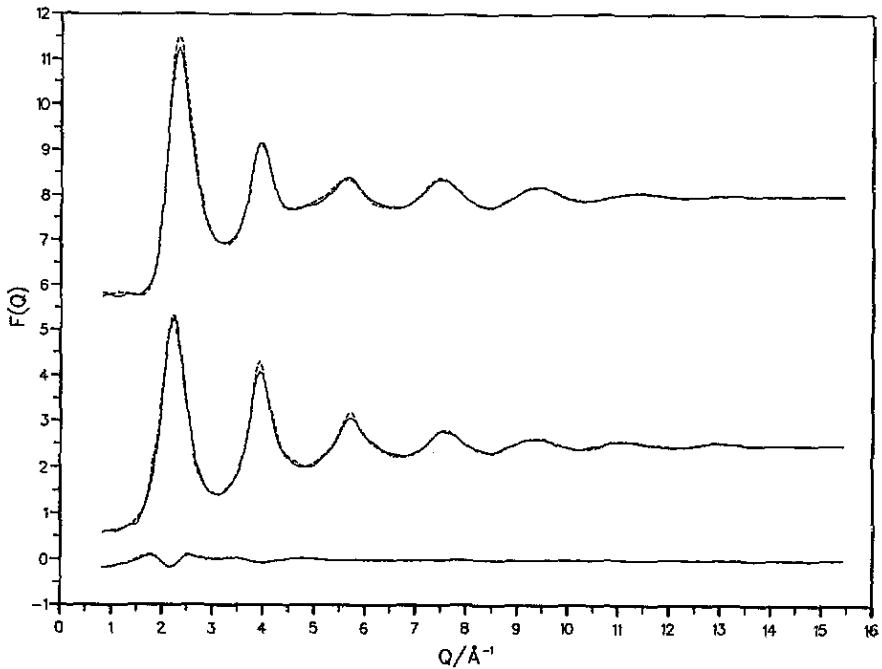


Figure 1. Total atomic structure factors for Dy_7Ni_3 with three different isotopic compositions; $^{14}\text{Dy}_7\ ^{14}\text{Ni}_3$ (top, shifted by 8.0), $^{14}\text{Dy}_7\ ^{15}\text{Ni}_3$ (centre, shifted by 2.0) and $^{15}\text{Dy}_7\ ^{14}\text{Ni}_3$ (bottom). Broken line, experimental data of Hannon *et al* 1991); solid line, RMC fit.

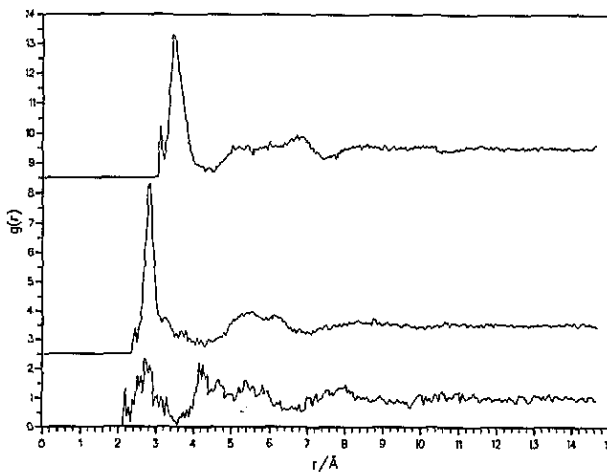


Figure 2. Partial radial distribution functions for Dy_7Ni_3 obtained by RMC modelling; $g_{\text{DyDy}}(r)$ (top, shifted by 8.5), $g_{\text{DyNi}}(r)$ (centre, shifted by 2.5) and $g_{\text{NiNi}}(r)$ (bottom).

arrangement of spins was used as the initial spin configuration for modelling the data at $T = 7\text{K}$. At higher temperatures the final configuration that had been fitted to the next lower temperature was then used as a starting configuration. A random arrangement of spins was also used as the initial configuration, fitting first to the 293 K data and then consecutively to the lower temperatures. The results were found to be

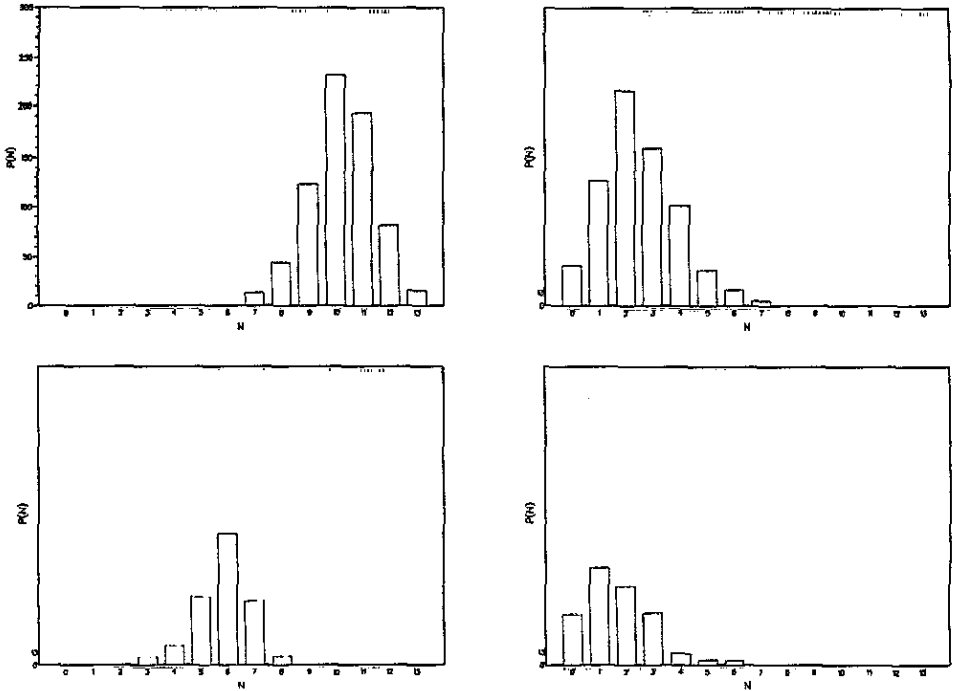


Figure 3. The distribution of number of neighbours within the appropriate first coordination shells of Dy_7Ni_3 ; Dy-Dy (top left), Dy-Ni (top right), Ni-Dy (bottom left) and Ni-Ni (bottom right).

independent of the initial configuration. RMC fits to the magnetic structure factors for ${}^0\text{Dy}_7{}^0\text{Ni}_3$ are shown in figure 5; again very good agreement has been obtained. The spin-spin correlation function may be calculated from the spin configurations

$$\langle \mu \cdot \mu' \rangle = n_\mu(r) / n_M(r) \quad (r > r_M^0) \quad (7)$$

where $n_M(r)$ is the number of magnetic atoms at a distance between r and $r + dr$ from a central magnetic atom, averaged over all magnetic atoms as centres, and r_M^0 is the distance of closest approach of two magnetic ions. Dividing by $n_M(r)$ removes the effect of the density of spins in $n_\mu(r)$. $\langle \mu \cdot \mu' \rangle$ is shown in figure 6 for each temperature. Angular correlations of neighbouring spins, $P_\mu(\cos\theta)$, may also be calculated from the configurations (figure 7). $P_\mu(\cos\theta)$ is defined as the number of spin pairs within the first coordination shell (as defined above) whose relative angles have cosines between $\cos\theta$ and $\cos\theta + \delta\cos\theta$.

4. Discussion of results

4.1. Atomic structure

The distribution of coordination numbers of Dy and Ni (figure 3) and the bond angle distributions (figure 4) are consistent with an atomic structure that is essentially a random close packed arrangement. Analysis of the bond angle distribution in terms of spherical harmonic invariants (see e.g. McGreevy and Pusztai 1990) indicates that

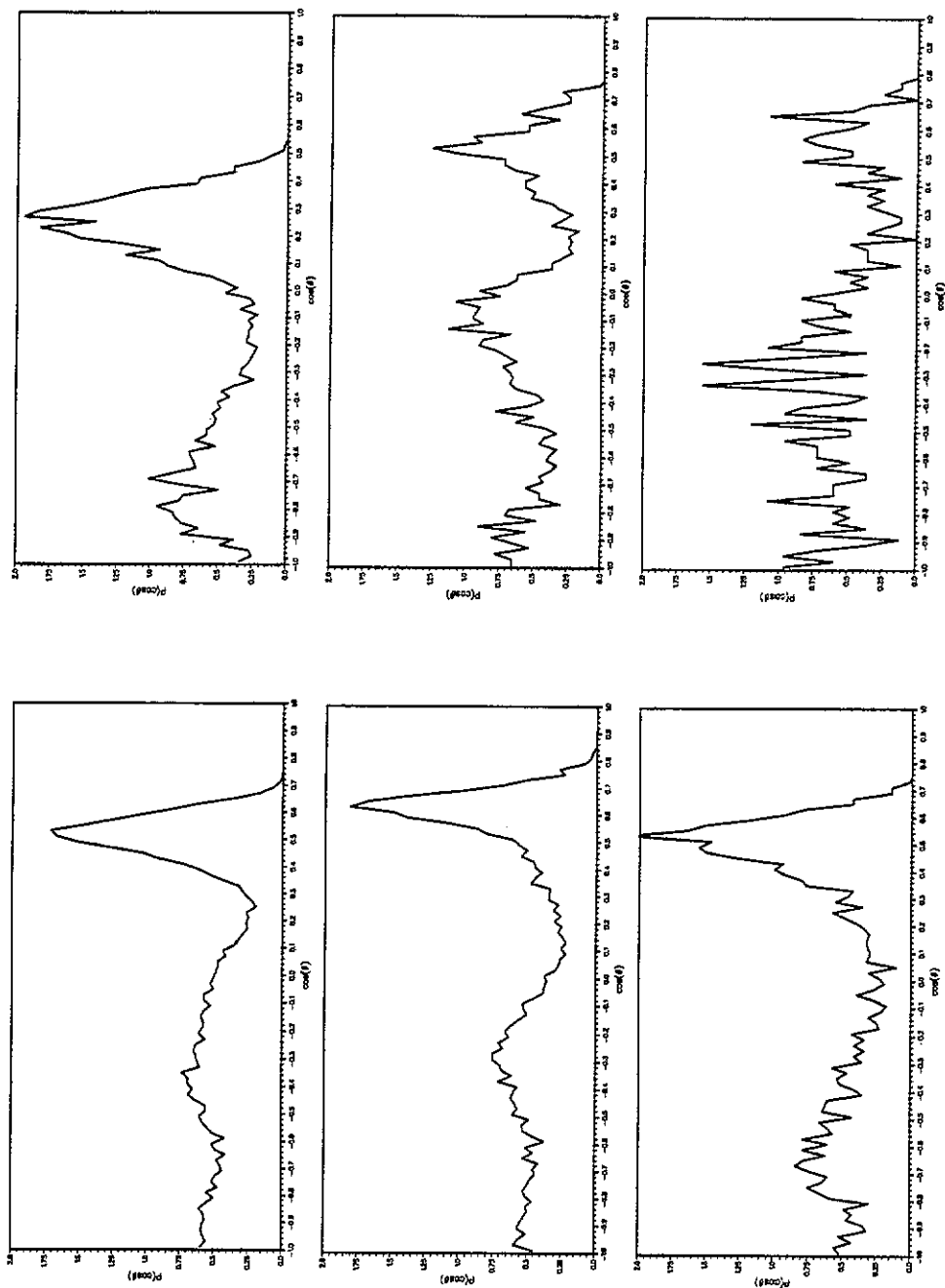


Figure 4. Bond angle distributions $P(\cos\theta)$ for Dy_7Ni_3 : Dy-Dy-Dy (top left), Dy-Ni-Dy (top right), Ni-Dy-Ni (centre left), Ni-Ni-Dy (bottom left) and Ni-Ni-Ni (bottom right).

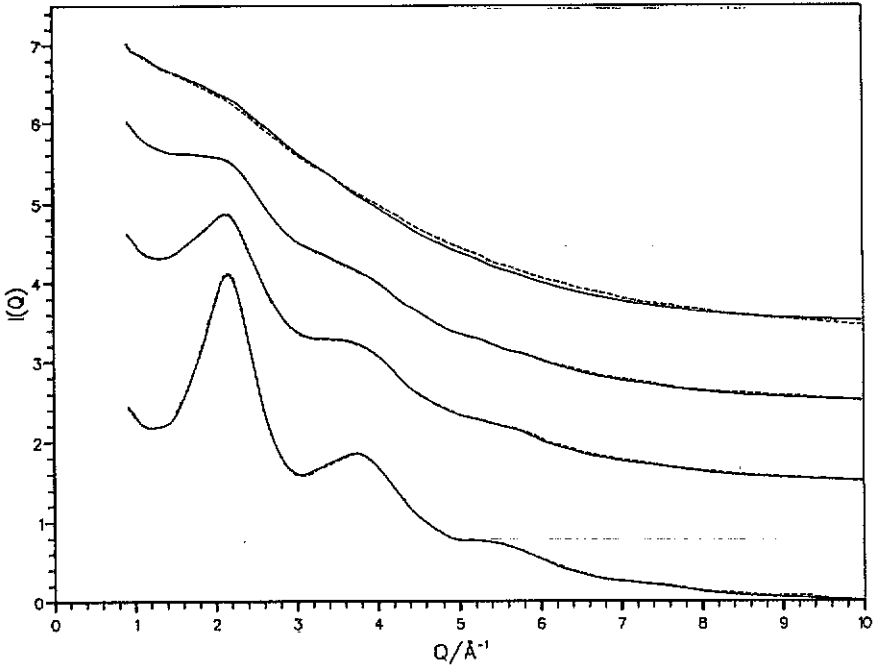


Figure 5. Total structure factors for ${}^0\text{Dy}_7{}^0\text{Ni}_3$ at $T = 7, 44, 96$ and 293 K (in ascending order, shifted by 0, 1.5, 2.5 and 3.5 respectively). Broken line, experimental data of Hannon *et al* (1991); solid line, RMC fit.

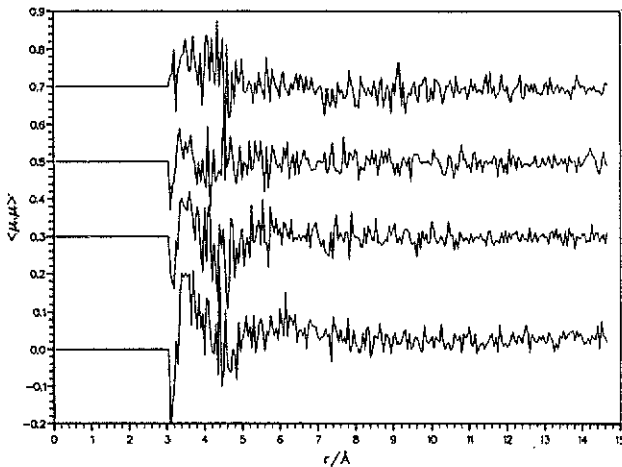


Figure 6. Spin-spin correlation function $\langle \mu_i \cdot \mu_j \rangle$ calculated from the RMC configurations for Dy_7Ni_3 at $T = 7, 44, 96$ and 293 K (in ascending order, shifted by 0, 0.3, 0.5 and 0.7 respectively).

the local symmetry is closest to hexagonal close packed, as it is for many simple liquid metals. There is no strong evidence of local structures similar to those found in crystalline Dy-Ni alloys. It is interesting to note that the simple close packed structure found here differs from the dominantly icosahedral arrangement found for

Ni-B and Fe-B glasses (Pusztai and McGreevy 1991).

4.2. Magnetic structure

At $T = 7$ K the spin correlation function $\langle \mu_i \cdot \mu_j \rangle'$ peaks positively at an r value corresponding to the first peak in $g_{DyDy}(r)$ (see figures 2 and 6), while $P_\mu(\cos\theta)$ peaks at $\cos\theta = 1$ (figure 7). This shows that the nearest neighbour magnetic interaction is predominantly ferromagnetic. However, because $P_\mu(\cos\theta)$ has a very broad peak and $\langle \mu_i \cdot \mu_j \rangle'$ displays r dependent structure, there is considerable deviation from ideal ferromagnetism and the magnetic correlations are more complex. (Ideal ferromagnetism would be characterized in $\langle \mu_i \cdot \mu_j \rangle'$ by a flat distribution.) Any long range ferromagnetic order is rapidly lost as the temperature is raised above the Curie temperature ($T_C = 40$ K, Buschow (1980)) such that $P_\mu(\cos\theta)$ is flat at $T = 96$ K, although the first peak in $\langle \mu_i \cdot \mu_j \rangle'$ is still slightly positive.

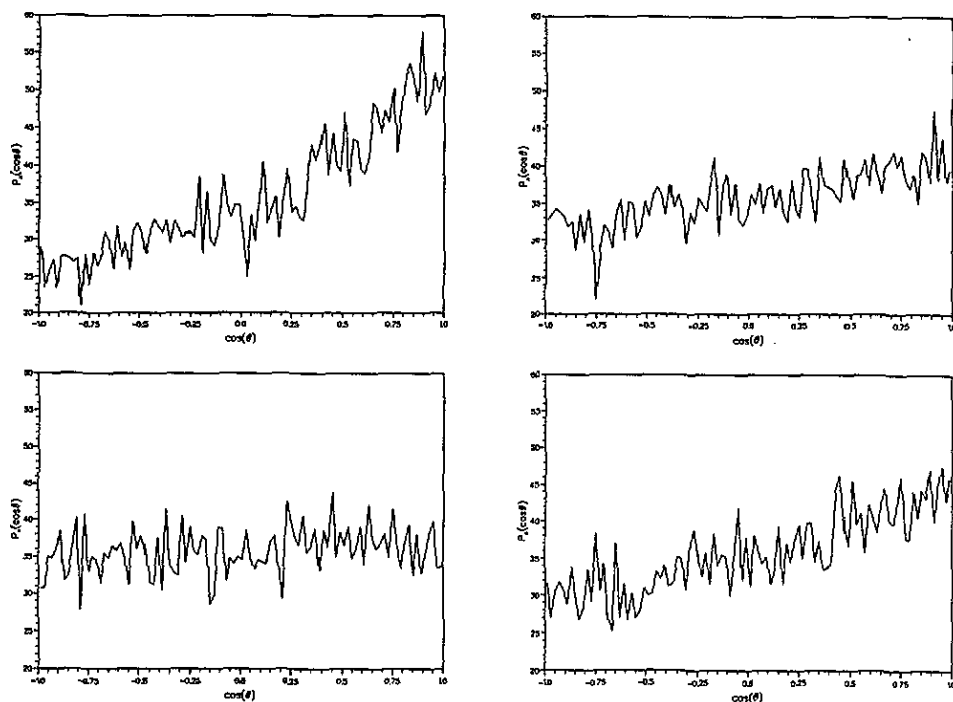


Figure 7. Angular correlation function $P_\mu(\cos\theta)$ between pairs of spins within the first Dy-Dy co-ordination shell for Dy_7Ni_3 at $T = 7$ K (top left), 44 K (top right), 96 K (bottom left) and 293 K (bottom right).

The macroscopic magnetization may be simply calculated from the configurations. This quantity has been measured experimentally by Buschow (1980) at a number of applied fields. From his work we estimate that the zero field magnetization should be approximately $1.9 \mu_B/Dy^{3+}$ ion at $T = 7$ K and zero for $T = 44, 96$ and 293 K. By introducing an extra term in the definition of χ^2 ,

$$\chi^2 = \sum_{i=1}^m [I^C(Q_i) - I^E(Q_i)]^2 / 2\sigma^2 + \alpha(M^C - M^E)^2 / 2\sigma_M^2 \quad (8)$$

the total magnetization of the simulation M^C may be constrained to the experimentally determined value M^E (α is a weighting factor). Investigations using the $T = 7\text{ K}$ data showed that constraining the total magnetization in this manner did not degrade the agreement with $I^E(Q)$ unless an unphysical value of M^E was used. A value of $M^E = 4.5 \mu_B/\text{Dy ion}$ (the magnetization at 4.2 K in a field of 18 kOe) produced a fit to the structure factor $\approx 5\%$ worse. The effect of constraining the total magnetization to larger than physical values was to increase the flat level of $\langle \mu \cdot \mu \rangle'$ and to make $P_\mu(\cos\theta)$ peak more sharply at $\cos\theta = 1$. In other words it makes the configuration more ferromagnetic, as would be expected. The data shown in figures 5-7 have the total magnetization constrained to the experimentally determined values.

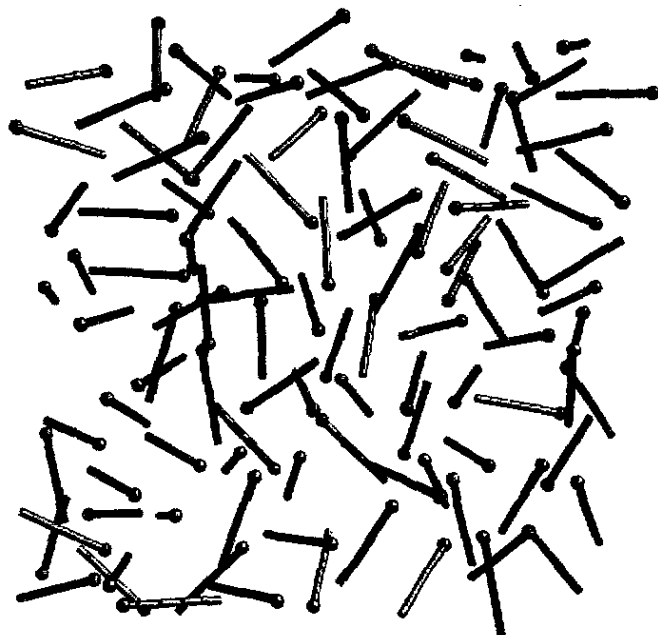


Figure 8. Spin distribution in a section of a configuration for Dy_7Ni_3 at 7 K. The direction of the macroscopic magnetization is almost exactly to the right and in the plane of the page.

In figure 8 we show the spin structure in a section of a configuration at $T = 7\text{ K}$. It is clear that the spin ordering is only weakly ferromagnetic. It should be noted at this point that the *mean* angle of spins with respect to the net magnetization axis is $\approx 80^\circ$, corresponding to a magnetization of $1.9 \mu_B/\text{Dy ion}$, but the *mode* of the angular distribution occurs at 0° . Any interpretation that the spins are 'canted', based on the average magnetization and hence on the *mean* of the spin angle, is therefore misleading.

The Q range of the available data limit the amount of information that may be gained from RMC modelling, especially with respect to any long-range magnetic order that may exist. The minimum Q is 0.9 \AA^{-1} and hence any correlations longer than 7 \AA cannot be reliably determined. To a large extent this limitation is compensated for by constraining the macroscopic magnetization, but lower Q data would obviously be valuable. Given that the use of large configurations (up to 30 000 atoms) is

possible data down to 0.2 \AA^{-1} can be used. In addition the magnetic form factor must be carefully chosen. Since the ${}^0\text{Dy}_7{}^0\text{Ni}_3$ data at room temperature are in the paramagnetic phase they should provide an accurate measurement of the Dy^{3+} form factor in Dy_7Ni_3 . However, because the data were not normalized and there is some evidence of structure (possibly from residual short range order) close to the same Q value where the 7 K data peaks most strongly, the tabulated values for the free ion form factor were used instead. This is not an ideal choice since the free ion form factor would not be expected to be correct for Dy^{3+} in Dy_7Ni_3 . Indeed this is shown in the RMC fits to the ${}^0\text{Dy}_7{}^0\text{Ni}_3$ data measured at $T = 293 \text{ K}$ where such a disparity in form factor would be expected to have, relative to the coherent magnetic scattering, the largest effect. The agreement with this data is not as good as at lower temperatures, and slightly spurious results were obtained such as a weak peak in $P_\mu(\cos\theta)$ at $\cos\theta = 1$ (figure 7). These problems would be alleviated with a more accurate experimental determination of the form factor.

5. Conclusions

We have shown that the RMC method may readily be used to model disordered magnetic structures as well as disordered atomic structures. The spin configurations produced agree quantitatively with the experimental data and may be used to describe the disordered magnetic structure. We have demonstrated this by fitting isotopic substitution neutron diffraction data for Dy_7Ni_3 , a magnetic amorphous alloy. The results obtained for both the atomic and magnetic structures are not only consistent with those determined by other methods, but also give a greater insight into the three-dimensional nature of these disordered structures. The ability to incorporate further experimental information in the simulation, e.g. macroscopic magnetization measurements, is clearly very useful and may readily be extended to include other known quantities.

Experimental separation of nuclear and magnetic scattering has, in the past, been required prior to analysis of disordered magnetic structures and a number of different methods have been employed. In spin glasses the nuclear scattering is largely confined to sharp Bragg peaks and the magnetic scattering to broad diffuse features so separation of the two is relatively straightforward. The magnetic scattering can often be isolated by subtraction of data measured at a temperature where paramagnetism is observed from data measured in the 'ordered' phase. Neutron polarization analysis may also be used (Moon *et al* 1968). In the case we have considered, double-null isotopic substitution was used. There are problems, however, in relying on experimentally separated nuclear and magnetic scattering. Some spin glasses display diffuse neutron scattering due to short range atomic order in similar regions of reciprocal space to the magnetic diffuse scattering, for example the crystalline alloy CuMn (Cable *et al* 1984). Polarization analysis is time consuming and intrinsically less accurate. For some amorphous materials the magnetic ordering temperature is too close to the crystallization temperature for a paramagnetic measurement to be possible. These complications may make rigorous separation of magnetic and nuclear scattering impossible by experimental means alone.

We are aware that merely showing that the RMC simulation technique is successful in modelling data obtained using double-null isotopic substitution does not demonstrate its general applicability. Indeed there are hardly any materials where such an

experimental technique is possible. However, because RMC can model the atomic and magnetic structures at the same time it does not require an experimental separation of the nuclear and magnetic scattering. The example which we have used in this paper did not involve moving atoms and rotating spins at the same time only because the data were such as to make it unnecessary. The RMC method can be used to model less complete data, or data from different experimental techniques. The ability to combine neutron diffraction, x-ray diffraction and EXAFS data (Keen and McGreevy 1990, Gurman and McGreevy 1990) and to constrain this with information such as the macroscopic magnetization, will mean that for almost all problems multiple data sets could be available. Modelling the combined data sets with RMC can elucidate the nuclear and magnetic structures and it is therefore widely applicable to the study of disordered magnetic structures.

Acknowledgments

We acknowledge the use of the neutron diffraction data of Hannon *et al* (1991) and useful discussions with A C Hannon. RLM thanks the Royal Society for continued support.

References

- Binder K and Young A P 1986 *Rev. Mod. Phys.* **58** 801
Blech I A and Averbach B L 1964 *Physics* **1** 31
Buschow K H J 1980 *J. Magn. Magn. Mater.* **21** 97
Cable J W, Werner S A, Felcher G P and Wakabayashi N 1984 *Phys. Rev. B* **29** 1268
Enderby J E, North D M and Egelstaff P E 1966 *Phil. Mag.* **14** 961
Faber T E and Ziman J M 1965 *Phil. Mag.* **11** 153
Fernández J F, Farach H A, Poole C P Jr and Puma M 1983 *Phys. Rev. B* **27** 4274
Fernández J F and Streit T S J 1982 *Phys. Rev. B* **25** 6910
Furdyna J K and Samarth N 1987 *J. Appl. Phys.* **61** 3526
Gurman S J and McGreevy R L 1990 *J. Phys.: Condens. Matter* **2** 9463
Hannon A C, Wright A C and Sinclair R N 1991 *Mater. Sci. Eng. A* **134** 883
Howe M A and McGreevy R L 1991 *Phys. Chem. Liq.* at press
Huang C Y 1985 *J. Magn. Magn. Mater.* **51** 1
Kasuya J 1956 *Prog. Theor. Phys.* **16** 45
Keen D A and McGreevy R L 1990 *Nature* **344** 423
Kittel C 1976 *Introduction to Solid State Physics* 5th edn (New York: Wiley) p 442
Lisher E J and Forsyth J B 1971 *Acta Crystallogr. A* **27** 545
McGreevy R L, Howe M A, Keen D A and Clausen K N 1990 *Neutron Scattering Data Analysis 1990* (*Inst. Phys. Conf. Ser.* **107**) ed M W Johnson (Bristol: Institute of Physics) p 165
McGreevy R L and Pusztai L 1988 *Mol. Simul.* **1** 359
— 1990 *Proc. R. Soc. A* **430** 241
Metropolis N, Rosenbluth A W, Rosenbluth M N, Teller A H and Teller E 1953 *J. Phys. Chem.* **21** 1087
Moon R M, Riste T and Koehler W C 1968 *Phys. Rev.* **181** 920
Moorjani K and Coey J M D 1984 *Magnetic Glasses* (Amsterdam: Elsevier)
Ruderman M A and Kittel C 1954 *Phys. Rev.* **96** 99
Sellmyer D J D, Nafis S and O'Shea M J 1988 *J. Appl. Phys.* **68** 3743
Wright A C 1980 *J. Non-Cryst. Solids* **40** 325
Wright A C, Hannon A C, Sinclair R N, Johnson W L and Atzmon M 1984 *J. Phys. F: Met. Phys.* **14** L201
Yosida K 1957 *Phys. Rev.* **106** 893